Mechanism of fusidic acid inhibition of RRF- and EF-G-dependent splitting of the bacterial post-termination ribosome

Anneli Borg, Michael Pavlov and Måns Ehrenberg*

Department of Cell and Molecular Biology, Biomedical Center, Uppsala University, Box 596, 75124 Uppsala, Sweden

ABSTRACT

The antibiotic drug fusidic acid (FA) is commonly used in the clinic against gram-positive bacterial infections. FA targets ribosome-bound elongation factor G (EF-G), a translational GTPase that accelerates both messenger RNA (mRNA) translocation and ribosome recycling. How FA inhibits translocation was recently clarified, but FA inhibition of ribosome recycling by EF-G and ribosome recycling factor (RRF) has remained obscure. Here we use fast kinetics techniques to estimate mean times of ribosome splitting and the stoichiometry of GTP hydrolysis by EF-G at varying concentrations of FA, EF-G and RRF. These mean times together with previous data on uninhibited ribosome recycling were used to clarify the mechanism of FA inhibition of ribosome splitting. The biochemical data on FA inhibition of translocation and recycling were used to model the growth inhibitory effect of FA on bacterial populations. We conclude that FA inhibition of translation provides the dominant cause of bacterial growth reduction, but that FA inhibition of ribosome recycling may contribute significantly to FA-induced expression of short regulatory open reading frames, like those involved in FA resistance.

INTRODUCTION

The GTPase elongation factor G (EF-G) has dual roles in bacterial protein synthesis (1). EF-G promotes translocation of the peptidyl-tRNA and the deacylated tRNA from the aminoacyl (A) and the peptidyl (P) to the P and exit (E) sites, respectively, and concomitantly of the messenger RNA (mRNA) by one codon in the ribosomal frame. Together with ribosome recycling factor (RRF), EF-G also promotes splitting of the post-termination ribosome into ribosomal subunits (2,3). The antibiotic fusidic acid (FA) inhibits protein synthesis by targeting ribosome-bound EF-G in both translocation and ribosome recycling (4). Since its discovery in the early 1960s, FA has been used to treat infections by gram-positive bacteria (5). Development of resistance among bacterial pathogens is an ever growing clinical concern and FA resistance is often conferred by mutations in the EF-G-encoding fusA gene (6,7) or by truncation or deletion of ribosomal protein L6 (8). In *Staphylococcus aureus* resistance is mainly conferred by the FusB protein which is expressed from the USB1 plasmid. FusB has been suggested to promote dissociation of EF-G from FA-stalled ribosome complexes and thereby reduce the growth inhibitory effect of the drug (9,10).

Early experiments showed that FA inhibits apo-ribosome-induced GTP hydrolysis cycles by EF-G with an inhibition constant (K_I-value), defined as the free FA concentration at which the steady state cycling rate is reduced by a factor of two, of 1 μM (11,12). FA decreases the rate of EF-G(GDP) dissociation from the ribosome (13) but leaves the rate of GTP hydrolysis upon EF-G(GTP) binding to the vacant ribosome unaltered (14). FA inhibits the peptide elongation cycle by targeting EF-G in three states of the ribosomal translocation process (15). Firstly, FA binds with high efficiency to EF-G in an early translocation state, from which the FA- and EF-G-bound ribosome proceeds to a drug-stalled intermediate translocation state. Secondly, FA may repeatedly bind to EF-G in this intermediate translocation state and thereby increase the ribosome stalling time in response to increasing FA concentration. Thirdly, FA may bind to EF-G in the post-translation state of the ribosome, thereby inhibiting dissociation of the factor after completed translocation. We have suggested that the first state corresponds to the pre-translocation ribosome with rotated subunits after GTP hydrolysis by EF-G, the second to a recent cryo-EM structure, visualized by Ramrath *et al.*, of a partially translocated complex (16) and the third to an X-ray structure, visualized by Gao *et al.*, of a post-translocation complex still bound to EF-G and FA (17). Under *in vivo*-relevant conditions, already at an FA concentration of 0.6 μM the peptide elongation cycle time is 2-fold of that for the uninhibited ribosome ($K_I = 0.6$ μM) (15), a K_I-value ~400 times smaller than a

*To whom correspondence should be addressed. Tel: +46 18 471 42 13; Fax: +46 18 471 42 62; Email: ehrenberg@xray.bmc.uu.se

previously reported K_I-value of 200 μM for FA-induced inhibition of translocation (4).

In the present work we have clarified the mechanism by which FA inhibits RRF- and EF-G-driven ribosome recycling (2,18,19). For this we used a stopped-flow instrument, with detection of Rayleigh light scattering to monitor the time-dependent extent of ribosome splitting, and a quench-flow instrument, for monitoring the time-dependent extent of GTP hydrolysis, at varying concentrations of FA, EF-G and RRF. This data set was used to construct a detailed kinetic model of FA inhibition of ribosome recycling for subsequent systems biology modelling of the impact of FA on bacterial growth. From this we were able to assess the relative impacts of FA inhibition of ribosome recycling and translocation (15) on the bacterial growth rate. In contrast to a previous proposal (4), we suggest that the FA-dependent inhibition of translocation provides the major growth inhibitory impact of the drug.

MATERIALS AND METHODS

Materials and reaction conditions

Ribosomes (*Escherichia coli* MRE600) were prepared according to Johansson *et al.* (20). His-tagged EF-G and RRF were overexpressed in *E. coli* and purified by nickel affinity chromatography. mRNA encoding the peptide fMet-Phe-Thr (sequence GGGAAUUCGGGCCCUUGUUAA-CAAUUAAGGAGGUAUUAA **AUG UUU ACG UAA** UUGCAGAAAAAAAAAAAAAAAAAAAAA (ORF in bold)) was prepared as described previously (15). tRNA^{Phe} was overexpressed in and purified from *E. coli*. [³H]-GTP was from Biotrend and unlabelled ATP and GTP were from GE Healthcare. FA sodium salt, phosphoenol pyruvate (PEP), puryvate kinase (PK), myokinase (MK) were from Sigma Aldrich. All other chemicals were from Merck or Sigma Aldrich.

All experiments were performed at 37°C in polymix buffer containing 95 mM KCl, 5 mM NH$_4$Cl, 0.5 mM CaCl$_2$, 8 mM putrescine, 1 mM spermidine, 5 mM potassium phosphate, 1 mM dithioerythritol and 5 mM Mg(OAc)$_2$.

Stopped-flow measurements of ribosome recycling in the presence of FA

A post-termination complex mixture was prepared containing GTP (1 mM), ATP (1 mM), PEP (10 mM), PK (50 μg/ml), MK (2 μg/ml), 70S ribosomes (0.5 μM), tRNA^{Phe} (2 μM), MFT mRNA (8 μM) and FA (0–200 μM, as indicated for each experiment). A recycling factor mixture was prepared containing GTP (1 mM), ATP (1 mM), PEP (10 mM), PK (50 μg/ml), MK (2 μg/ml), IF3 (16 μM), RRF (2–40 μM) and EF-G (1–20 μM, active concentration determined as in (15)). The two mixtures were incubated at 37°C for 15 min and then centrifuged at 20 800×g for 3 min. They were rapidly mixed in a stopped-flow instrument (Applied Photophysics SX20) at 37°C and the real-time decrease in light scattering intensity was recorded at 436 nm.

Determination of the number of GTP molecules hydrolyzed per recycling event in the presence of FA

A post-termination complex mixture was prepared containing ATP (1.96 mM), PEP (10 mM), 70S ribosomes (2 μM), tRNA^{Phe} (5 μM), MFT mRNA (10 μM), [³H]-GTP (40 μM) and FA (0–150 μM). A recycling factor mixture was prepared containing ATP (2 mM), PEP (10 mM), IF3 (24 μM), RRF (60 μM), EF-G (1.0 μM, active concentration) and FA (0–150 μM). The two mixtures were incubated at 37°C for 15 min. To monitor the GTP hydrolysis reaction, equal volumes of the post-termination complex mixture and the recycling factor mixture were rapidly mixed in a quench-flow instrument and the reaction quenched after different incubation times by mixing with 50% formic acid. Precipitates were removed by centrifugation and the supernatant analysed by HPLC as described in (15). To monitor the ribosome splitting equal volumes of the post-termination complex mixture and the recycling factor mixture were rapidly mixed in a stopped-flow instrument and the splitting reaction monitored by light scattering as described above.

RESULTS

The mechanism of FA-dependent inhibition of ribosome recycling

The recently clarified mechanism of EF-G- and RRF-promoted recycling of the bacterial ribosome (19) is shown as the FA-independent part of the scheme in Figure 1. The definitions of its parameters and their experimentally estimated values are displayed in Tables 1 and 2. This mechanism (19) was established from estimates of the mean ribosome recycling time, τ_{rec}, in stopped-flow experiments, where post-termination 70S ribosomes were rapidly mixed with EF-G and RRF. The time course of ribosome splitting into subunits was quantified by the decrease in Rayleigh light scattering with increasing incubation time. The dependence of τ_{rec} on the concentrations of RRF and EF-G was accounted for by five constants, the "A-parameters":

$$\tau_{rec} = A_1 + A_2 \frac{1}{[\text{RRF}]} + A_3 \frac{[G]}{[\text{RRF}]} + A_4 \frac{1}{[G]} + A_5 \frac{1}{[\text{RRF}][G]} \ (1)$$

The A-parameters were estimated by fitting τ_{rec} in Equation (1) to experimental estimates of ribosome splitting times at different concentrations of EF-G and RRF ((19), Table 1). These estimates, together with additional experiments, were then used to estimate the elemental rate constants and Michaelis–Menten parameters pertinent to the recycling mechanism (Figure 1, Table 2) as previously described (19).

To include the inhibitory action of FA in the model for ribosome recycling, we tentatively assumed that FA attacks EF-G(GDP) in complex with both RRF-free and RRF-bound post-termination ribosomes (Figure 1). The RRF-free complex had inferential support from multi-cycle experiments in which GTP hydrolysis by EF-G, stimulated by apo-ribosomes, was inhibited by slow release of FA from EF-G(GDP) on the ribosome (13). However, the RRF-bound complex lacked previous experimental support.
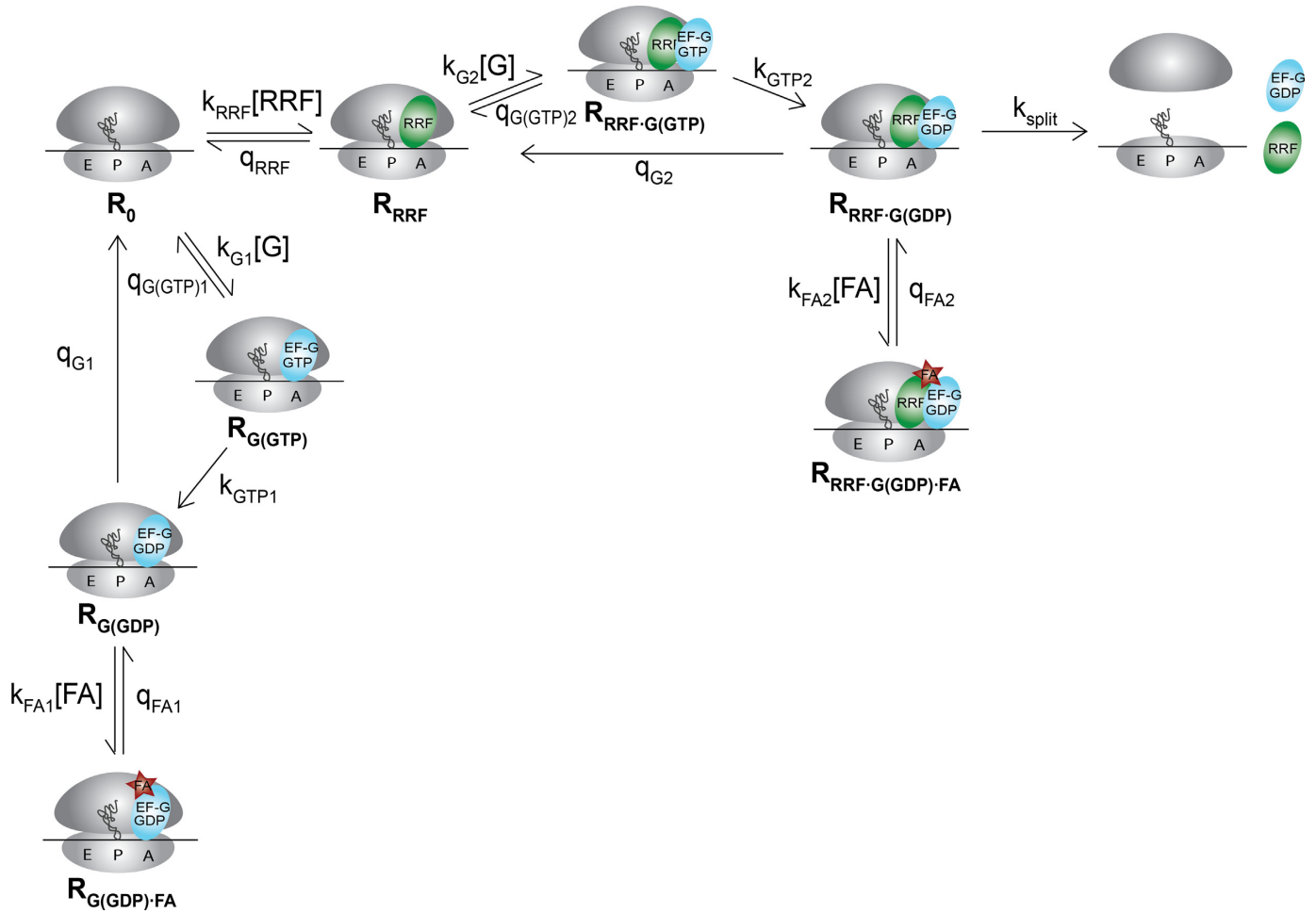
Figure 1. The complete kinetic mechanism for ribosome recycling in the presence of FA. RRF binds to the post-termination complex with rate constant k_{RRF} and dissociates with rate constant q_{RRF}. EF-G binds to the RRF-free ($X = 1$) or the RRF-bound ($X = 2$) post-termination complex with rate constant k_{GX}. EF-G(GTP) can then either dissociate with rate constant $q_{G(GTP)X}$ or hydrolyze GTP with rate constant k_{GTPX}. After GTP hydrolysis EF-G(GDP) dissociates with rate constant q_{GX}. FA binds to the EF-G-bound post-termination complex with rate constant k_{FA1} and to the EF-G- and RRF-bound post-termination complex with rate constant k_{FA2}. From both complexes it dissociates slowly, with rate constants q_{FA1} and q_{FA2}, respectively. Splitting of the RRF- and EF-G-bound post-termination complex occurs with rate constant k_{split}, also when it has been FA-bound and the drug has dissociated.

Table 1. A-parameters and the derived Q-parameter obtained by fitting of Equations (1) and (2) to recycling time data obtained in the presence (this study) and in the absence of FA (19)

Parameter	Definition	Value
A_1	$\frac{1}{k_{split}} + \frac{1}{k_{GTP2}}(1 + \frac{q_{G2}}{k_{split}})$	0.045 ± 0.023 s
A_2	$\frac{1}{k_{RRF}} + \frac{q_{RRF}}{k_{RRF}(k_{cat}/K_M)_{G2}(K_M)_{G1}}(1 + \frac{q_{G2}}{k_{split}})$	0.97 ± 0.13 s·μM
A_3	$\frac{1}{k_{RRF}(K_M)_{G1}}$	0.150 ± 0.020 s
A_4	$\frac{1}{(k_{cat}/K_M)_{G2}}(1 + \frac{q_{G2}}{k_{split}})$	0.138 ± 0.019 s·μM
A_5	$\frac{q_{RRF}}{k_{RRF}(k_{cat}/K_M)_{G2}}(1 + \frac{q_{G2}}{k_{split}})$	0.60 ± 0.11 s·μM^2
A_6	$\frac{(k_{cat}/K_M)_{G1}}{q_{FA1} K_{I1} k_{RRF}}$	0.554 ± 0.071 s·μM^{-1}
A_7	$\frac{1}{q_{FA2} K_{I2}}$	0.296 ± 0.051 s·μM^{-1}
Q	$\frac{q_{RRF}}{(k_{cat}/K_M)_{G2}}(1 + \frac{q_{G2}}{k_{split}}) = \frac{A_2}{2 A_3} + \sqrt{\left(\frac{A_2}{2 A_3}\right)^2 - \frac{A_5}{A_3}}$	6.2 ± 1.7 μM

Table 2. Rate and equilibrium constants related to ribosome recycling and its inhibition by FA

Parameter	Definition	Value
$(k_{cat}/K_M)_{G1}$ *	k_{cat}/K_M for the binding of EF-G(GTP) to the RRF-free post-termination ribosome ($= k_{G1}\cdot k_{GTP1}/(k_{GTP1}+q_{G(GTP)1})$)	$63 \pm 3\ \mu M^{-1}\ s^{-1}$
$(k_{cat})_{G1}$ *	k_{cat}-value for the cycling of EF-G on the RRF-free post-termination ribosome ($= q_{G1}\cdot k_{GTP1}/(q_{G1}+k_{GTP1})$)	$36.0 \pm 0.3\ s^{-1}$
$(K_M)_{G1}$ *	K_M-value for the binding of EF-G to the RRF-free post-termination ribosome ($= q_{G1}(k_{GTP1}+q_{G(GTP)1})/(k_{G1}(q_{G1}+k_{GTP1}))$)	$0.56 \pm 0.02\ \mu M$
k_{RRF} *	Second order rate constant for the binding of RRF to the post-termination ribosome	$15 \pm 3\ \mu M^{-1}\ s^{-1}$
q_{RRF} *	First order rate constant for the release of RRF from the post-termination ribosome	$58 \pm 7\ s^{-1}$
K_{RRF} *	Equilibrium constant for binding of RRF to the post-termination ribosome ($= q_{RRF}/k_{RRF}$)	$3.9 \pm 0.8\ \mu M$
$(k_{cat}/K_M)_{G2}$ *	k_{cat}/K_M for the binding of EF-G(GTP) to the RRF-bound post-termination ribosome ($= k_{G2}\cdot k_{GTP2}/(k_{GTP2}+q_{G(GTP)2})$)	$8.1 \pm 0.7\ \mu M^{-1}\ s^{-1}$
$1+q_{G2}/k_{split}$ *	The minimal number of GTP molecules consumed per splitting event at high RRF concentrations	1.1 ± 0.1
k_{max} *	The maximal rate of ribosome recycling ($= k_{GTP2}\cdot k_{split}/(k_{GTP2}+k_{split}+q_{G2})$)	$25 \pm 4\ s^{-1}$
q_{FA1}	Dissociation rate constant for FA from the EF-G-bound post-termination ribosome	$0.17 \pm 0.03\ s^{-1}$
K_{I1}	Inhibition constant for the binding of FA to the EF-G-bound post-termination ribosome ($= q_{G1}/k_{FA1}$)	$13 \pm 14\ \mu M$
q_{FA2}	Dissociation rate constant for FA from the RRF- and EF-G-bound post-termination ribosome	$0.18 \pm 0.08\ s^{-1}$
K_{I2}	Inhibition constant for the binding of FA to the RRF- and EF-G-bound post-termination ribosome ($= k_{split}/k_{FA2}$)	$19 \pm 7\ \mu M$

Parameters marked with an asterisk (*) are from (Borg *et al.* 2015 (19)).

The model in Figure 1 implies, firstly, that EF-G and FA act as competitive inhibitors of RRF binding to the post-termination complex. That is, FA binds to the already EF-G-bound post-termination ribosome, $R_{G(GDP)}$, with rate constant k_{FA1} to form a long-lived, recycling deficient complex, which decomposes slowly by release of FA with rate constant q_{FA1}. This reaction sequence, in which EF-G and FA bind to the RRF-free ribosome, is favoured by high concentrations of EF-G and FA and disfavoured by high concentration of RRF. Secondly, the model implies that FA also inhibits ribosome recycling by forming yet another long-lived complex by binding to the RRF- and EF-G-containing post-termination complex, $R_{RRF\cdot G(GDP)}$, with second-order rate constant k_{FA2}. At this point, ribosome splitting requires release of FA from the complex $R_{RRF\cdot G(GDP)\cdot FA}$ with rate constant q_{FA2} which is slow compared to the fast splitting, with rate constant k_{split}, in the uninhibited case. According to this model (Figure 1) the average recycling time in the presence of FA, τ_{recFA}, is given by (see Supporting Material, Equations (S2) and (S3)):

$$\tau_{recFA}=\tau_{rec}+\tau_{recI}=\tau_{rec}+(Q+[G])\cdot A_6\frac{[FA]}{[RRF]}+A_7[FA] \quad (2)$$

where A_6, A_7 and Q are constants and Q depends on parameters A_2, A_3 and A_5 through:

$$Q = A_2/2A_3 + \sqrt{(A_2/2A_3)^2 - A_5/A_3} \quad (3)$$

How $A1$ to $A7$ and Q depend on elemental rate constants and Michaelis-Menten parameters (Figure 1) is shown in Table 1.

All seven independent A-parameters in Equation (2) can be estimated from ribosome recycling experiments in which the concentrations of EF-G, RRF and FA are varied, as discussed below. First, however, we will demonstrate that the previously unidentified complex $R_{RRF\cdot G(GDP)\cdot FA}$ does in-

deed exist and that FA-dissociation from this complex directly brings it back to the splitting competent $R_{RRF\cdot G(GDP)}$-complex in Figure 1.

FA stalls the post-termination ribosome in complex with EF-G and RRF

The inhibition mechanism in Figure 1 postulates FA binding to EF-G on RRF-free as well as on RRF-bound ribosomes. Binding of FA to EF-G on the RRF-free ribosome is accounted for by those terms in Equation (2) that depend linearly on the [FA]/[RRF] concentration ratio, while binding of FA to EF-G on the RRF-containing ribosome is accounted for by the term linear in the FA concentration ($A_7[FA]$). According to Equation (2) a plot of τ_{recFA} versus the FA concentration at constant [FA]/[RRF] ratio would give a straight line with positive slope A_7 and positive y-axis intercept. For such an experiment, we prepared one mixture, containing FA (50–200 μM) and post-termination ribosomes (1 μM) with mRNA and deacylated P-site tRNA, and another mixture, containing FA (50–200 μM), EF-G (10 μM), IF3 (16 μM) and RRF, always fulfilling [FA]/[RRF] = 5. IF3 was present to prevent rejoining of the ribosomal subunits after 70S ribosome splitting. Equal volumes of the two mixtures were rapidly mixed in a stopped-flow instrument and the decreasing fraction of 70S ribosomes was monitored by Rayleigh light scattering (Figure 2A) as described previously (19). The time evolution of the light scattering curves displayed slow single phase kinetics and τ_{recFA}-values were estimated by fitting each time trace to a single exponential function ($a_0\cdot e^{-t/\tau_{recFA}}+bg$). As predicted, the recycling time, τ_{recFA}, increased linearly with the FA concentration (Figure 2B) and the A_7 parameter was estimated as 0.14 ± 0.05 s·μM^{-1} from the slope, while the y-axis intercept was estimated as 92 ± 6 s. This result confirms the existence of an FA-stalled post-termination com-
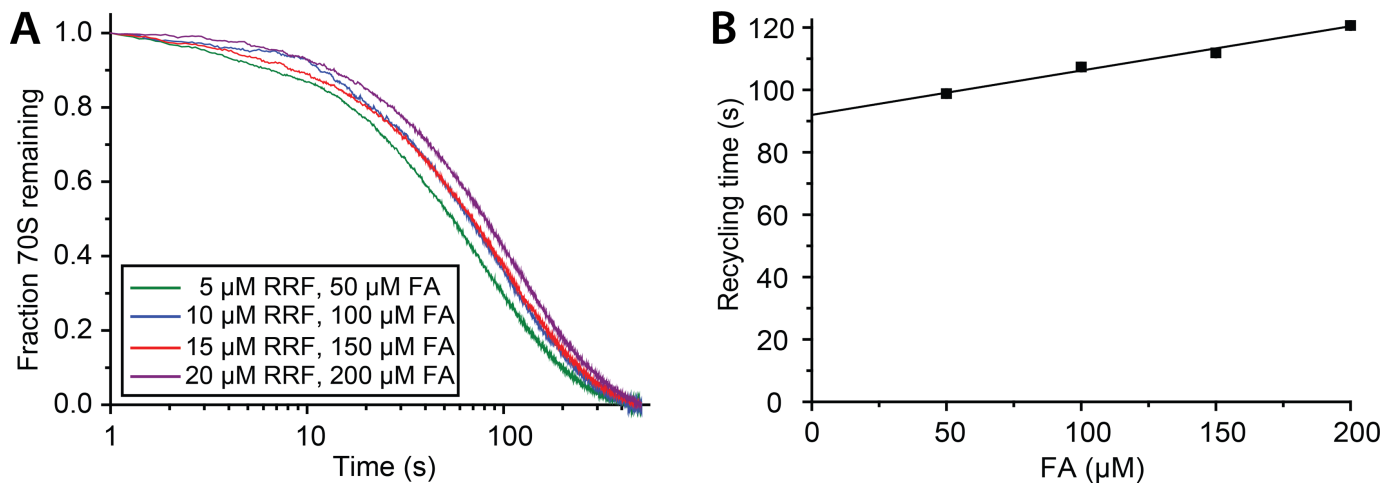
Figure 2. Ribosome recycling at constant [FA]/[RRF] concentration ratio. (**A**) Time traces for ribosome splitting recorded in the stopped-flow instrument at 5.1 μM EF-G and varying concentrations of RRF (5–20 μM) and FA (50–200 μM), the FA concentration in all cases 10-fold higher than the RRF concentration. The fraction of post-termination complexes remaining is plotted as a function of time. (**B**) Average splitting times obtained at constant [FA]/[RRF] concentration ratio determined by single exponential fitting of the time traces in A, plotted against the FA concentration. Fitting of a straight line estimated the intercept as 92 ± 6 s and the slope as 0.14 ± 0.05.

plex, $R_{\text{RRF·G(GDP)·FA}}$, containing both RRF and EF-G (Figure 1).

The average number of GTP molecules per ribosome splitting does not vary with the FA concentration

Although the titration experiment in the previous section corroborated the existence of $R_{\text{RRF·G(GDP)·FA}}$, it did not reveal whether dissociation of FA from this complex resulted in a splitting competent $R_{\text{RRF·G(GDP)}}$ complex (Figure 1). The possibility remained that RRF could dissociate before FA from $R_{\text{RRF·G(GDP)·FA}}$ leading to the $R_{\text{G(GDP)·FA}}$ complex or that $R_{\text{RRF·G(GDP)·FA}}$ could undergo a conformational change so that the complex formed upon FA dissociation was not splitting competent. We note that in both these scenarios the GTP consumption per successful splitting reaction would increase strongly with the FA concentration since EF-G release and rebinding would then be required to achieve ribosome splitting. In contrast, our model predicts the GTP consumption per splitting event, f_{GTP}, to be independent of the FA concentration as given by the previously derived expression for f_{GTP} in the absence of FA (19):

$$f_{\text{GTP}} = \frac{(k_{\text{cat}}/K_M)_{\text{G1}}}{k_{\text{RRF}}[\text{RRF}]} \left(\frac{q_{\text{RRF}}}{(k_{\text{cat}}/K_M)_{\text{G2}}} \left(\frac{q_{\text{G2}}}{k_{split}}+1 \right) + [G] \right) + \frac{q_{\text{G2}}}{k_{split}} + 1 \quad (4)$$

To estimate the GTP consumption per ribosome splitting event at different FA concentrations we prepared one mixture, containing post-termination ribosome complexes (2 μM), [³H]-GTP (40 μM) and FA (0–150 μM) and another, containing RRF (60 μM), EF-G (1 μM), IF3 (24 μM) and FA (0–150 μM). Equal volumes of the two mixtures were rapidly mixed in the stopped-flow instrument and the time-dependent decrease in 70S ribosome concentration was estimated from the change in Rayleigh light scattering intensity (Figure 3A), as described previously (19). To determine the concentration of GDP formed by GTP hydrolysis, equal volumes of the same two mixtures were rapidly mixed in a quench-flow instrument and the reaction quenched with formic acid after different incubation

times. The number of GTPs consumed per ribosome splitting was at each FA concentration estimated from the ratio between the concentrations of hydrolyzed GTP (Figure 3B) and split ribosomes (Figure 3A) and plotted as a function of time (Figure 3C). The stoichiometry ratio increased linearly with time due to GTP-hydrolysis by EF-G on the free 50S subunits that were formed during the splitting reaction (19). For each FA concentration the data points were fitted to a straight line and the zero time GTP-per-splitting stoichiometry, reflecting GTP hydrolysis in the absence of the 50S-induced side reaction, was estimated as the intercept with the y-axis (Figure 3C). The GTP consumption per ribosome splitting event was constant and close to 3.5 in the 0–150 μM FA concentration range, in accordance with the stoichiometry suggested by the recycling model for the uninhibited reaction (19) at the same RRF and EF-G concentrations. It follows that the $R_{\text{RRF·G(GDP)·FA}}$ complex remained splitting-competent also after FA binding so that, upon FA dissociation, it was rapidly split into subunits with high probability (Figure 1). This result also rules out the possibility that RRF could dissociate from $R_{\text{RRF·G(GDP)·FA}}$ before FA, to yield an $R_{\text{G(GDP)·FA}}$ complex.

Recycling time variation with the FA concentration at different concentrations of RRF and EF-G

According to Equations (1) and (2) the dependence of the average ribosome splitting time, τ_{recFA}, on the concentrations of RRF, EF-G and FA is accounted for by seven independent A-parameters. For precise estimates of these parameters we used stopped-flow technique in conjunction with Rayleigh light scattering to monitor the fraction of post-termination ribosomes remaining at different incubation times after rapid addition of RRF, EF-G and FA at different concentrations. For this, we prepared one mixture, containing post-termination ribosome complexes (0.5 μM) and FA (0–50 μM), and another mixture, containing RRF (2–20 μM), EF-G (2–20 μM), IF3 (16 μM) and FA (0–50
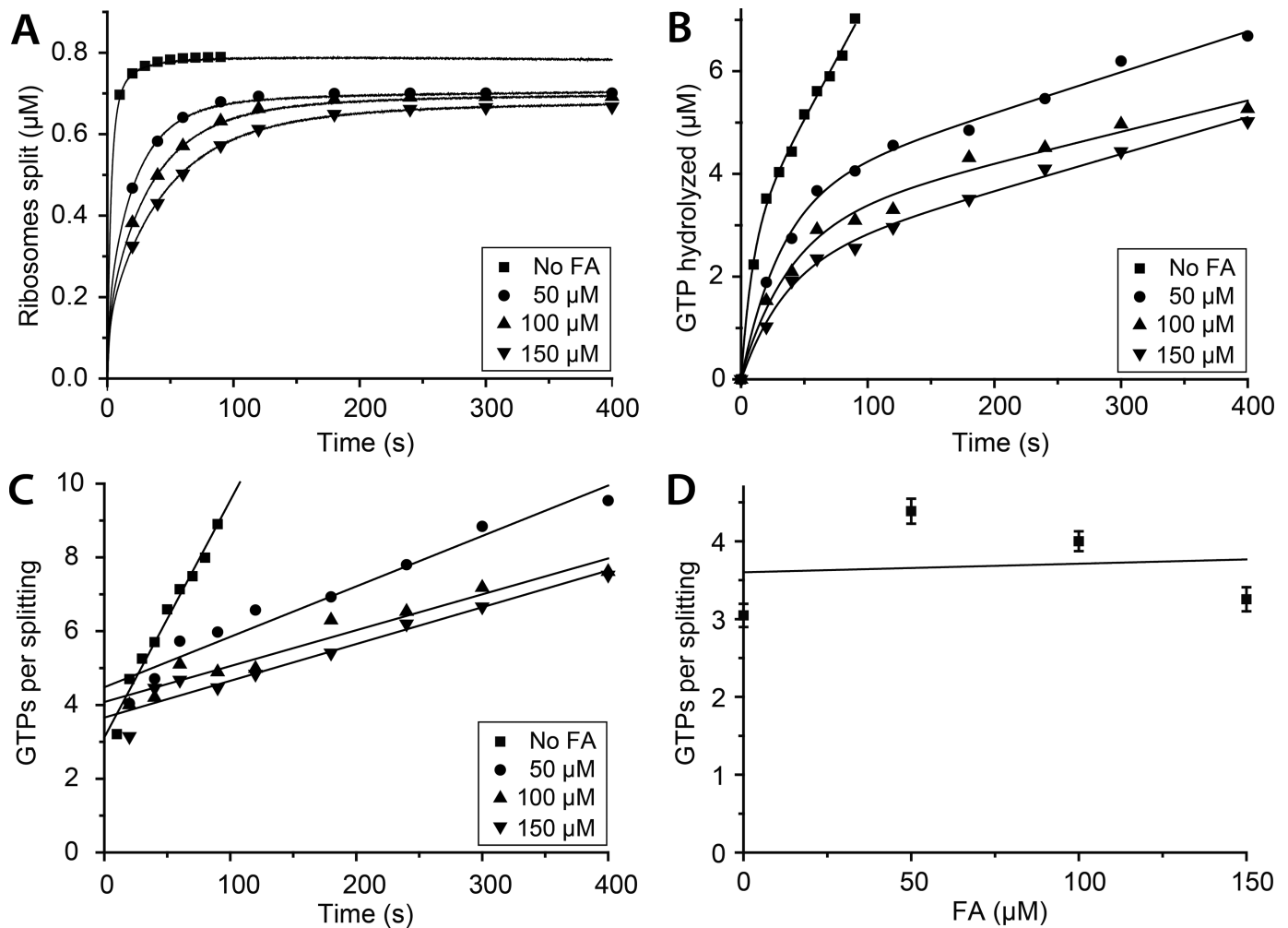
Figure 3. GTP consumption in ribosome recycling in the presence of FA. (**A**) Time curves of splitting of post-termination complexes (1 μM) obtained at 0.5 μM EF-G, 20 μM [^{3}H]-GTP, 30 μM RRF and varying concentrations of FA (0–150 μM). For each FA concentration the concentration of split ribosomes was plotted as a function of time. The points indicate the amount of split ribosomes after different times of incubation as calculated from two-exponential fits of the splitting time traces. (**B**) Time curves of GTP hydrolysis obtained under the same conditions as in A. For each FA concentration the concentration of hydrolyzed GTP was plotted as a function of time. The fitted lines are the sum of a single exponential and a straight line and are just indicative as it was the extent of GTP hydrolysis measured at different times of incubation, as indicated by the points, that was used for further analysis. (**C**) The ratio of the concentration of hydrolyzed GTP in B and the concentration of split ribosomes in A plotted as a function of time for each FA concentration. Straight lines were fitted to the data points to estimate the intercepts as the number of GTP molecules consumed per ribosome splitting event. The slopes reflect GTP hydrolysis by EF-G on 50S subunits formed in the recycling reaction, which is also inhibited by FA as seen from the decreasing slope with increasing FA concentration. (**D**) The number of GTP molecules hydrolyzed per splitting event plotted as a function of the FA concentration. The GTP consumption was essentially invariant with the FA concentration with a consumption of an average of 3.5 GTP molecules per ribosome splitting event.

μM). Equal volumes of the two mixtures were rapidly mixed in a stopped-flow instrument and Rayleigh light scattering was used to monitor the fraction of 70S ribosomes remaining at different incubation times, as exemplified in Figure 4A. We used curve fitting to estimate the total (τ_{recFA}) and uninhibited (τ_{rec}) recycling times for each curve (Equation (S4)). It is seen that τ_{recFA} was linear in the FA concentration for all three combinations of RRF and EF-G concentrations, as prescribed by Equation (2) (Figure 4D). We determined all seven A-parameters in the model for τ_{recFA} by fitting Equations (1) and (2) to the experimentally estimated recycling times in the absence (19) and presence (Figures 2B and 4D) of FA and the result is shown in Table 1. These seven parameters completely describe the increase in ribosome splitting time with increasing FA concentration Equa-

tions (1) and (2) for all combinations of EF-G and RRF concentrations. The A-parameters therefore determined the sensitivity parameter, K_I, for the FA-dependent rate of ribosome recycling at different RRF and EF-G concentrations, as described in the next section.

The sensitivity of ribosome recycling to the FA concentration depends on the RRF and EF-G concentrations

Equations (1) and (2) predict τ_{recFA}/τ_{rec} to be a linear function of the FA concentration with slope $1/K_I$, where the inhibition constant, K_I, is defined as the concentration of FA required to double the ribosome recycling time:

$$\tau_{recFA} = \tau_{rec} + \tau_{recI} = \tau_{rec}(1 + [FA]/K_I), \qquad (5)$$
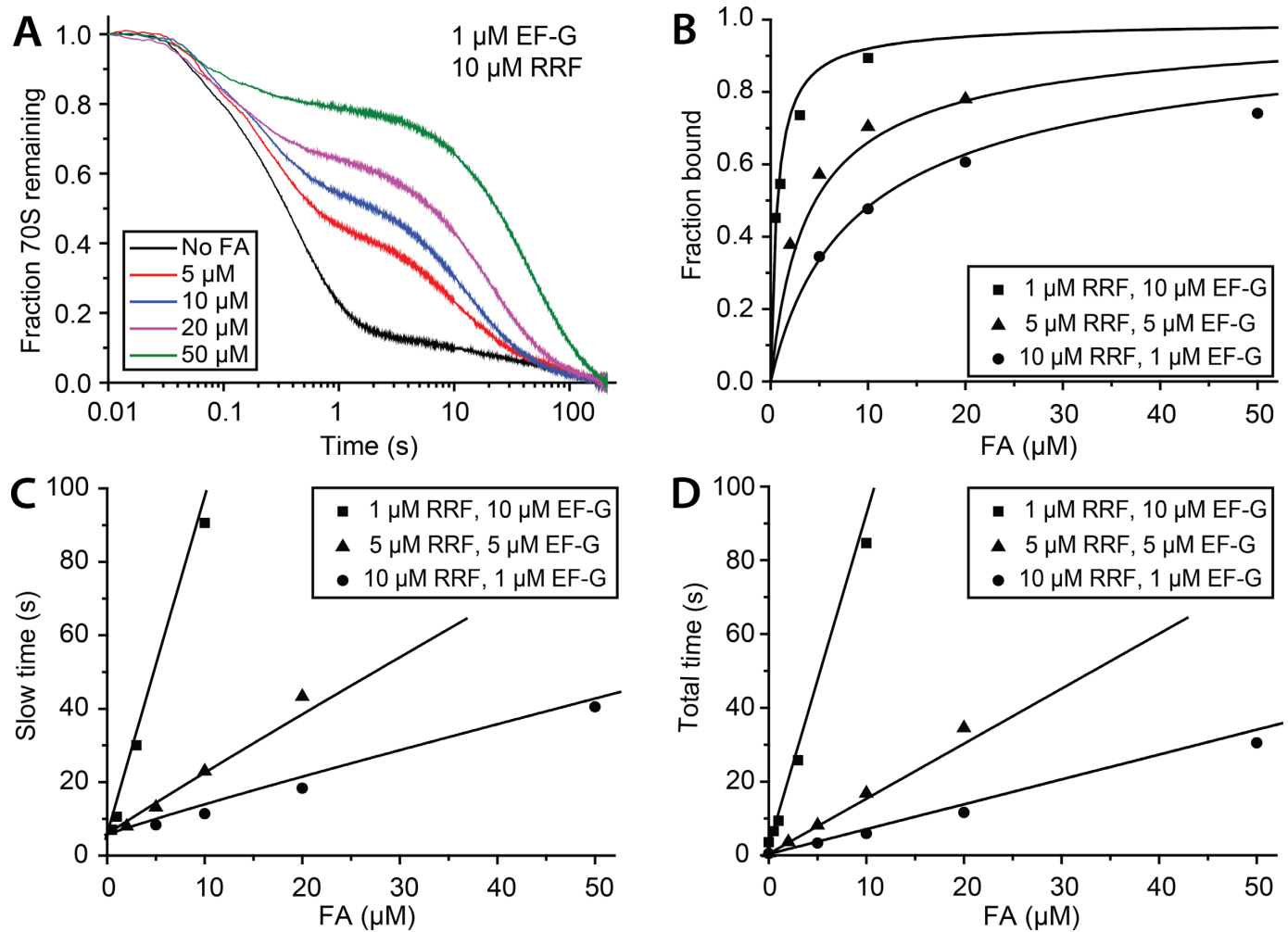
Figure 4. FA titration in ribosome recycling. (**A**) Time traces of ribosome recycling recorded in the stopped-flow instrument at 1 μM EF-G, 10 μM RRF and varying concentrations of FA (0–50 μM). The fraction of post-termination complexes remaining was plotted as a function of time. (**B**) The fraction of ribosomes that bind FA during ribosome recycling (p_I) at three different combinations of RRF and EF-G concentrations plotted as a function of the FA concentration. (**C**) Average time of the slow phase (τ_I) plotted as a function of the FA concentration. The intercepts indicate the average FA release time after a single binding event. The non-variability of the intercept for the different combinations of EF-G and RRF concentrations reflects the similarity in dissociation rate constant of FA from ribosome-bound EF-G in the presence or absence of RRF. (**D**) The total time of ribosome splitting (τ_{recFA}) plotted as a function of the FA concentration.

where

$$K_I = \frac{\tau_{rec}}{(\tau_{recI}/[FA])} =$$

$$\frac{A_1 + A_2 \frac{1}{[RRF]} + A_3 \frac{[G]}{[RRF]} + A_4 \frac{1}{[G]} + A_5 \frac{1}{[RRF][G]}}{\frac{A_6}{[RRF]}(Q + [G]) + A_7} \quad (6)$$

Equation (6) shows how the K_I-value depends on the free concentrations of EF-G and RRF both through the uninhibited recycling time, τ_{rec} (the numerator), and the per molar recycling time increase due to FA inhibition, $\tau_{recI}/[FA]$ (the denominator). Using the *A*-parameter values in Table 1 we estimated the K_I-values for the combinations of RRF and EF-G concentrations used in Figure 4 as 0.26 μM for 1 μM RRF and 10 μM EF-G, as 0.28 μM for 5 μM RRF and 5 μM EF-G and as 0.52 μM for 1 μM EF-G and 10 μM RRF. According to Equation (6) the K_I-value asymptotically approaches a value equal to $A_1/A_7 = 0.17$ μM,

when the concentrations of RRF and EF-G go to infinity and when, at the same time, the ratio between the RRF and EF-G concentrations increases indefinitely. A more physiologically relevant K_I-value is 0.29 μM, valid at free factor concentrations close to those in the living cell: 4 μM EF-G and 15 μM RRF (19). The K_I-value response to varying concentrations of EF-G and RRF is illustrated graphically in Figure 5.

The biphasic nature of FA-inhibited ribosome recycling

It was observed that inhibition of mRNA translation by FA leads to biphasic kinetics: there is a slow phase with an amplitude that increases and a fast phase with an amplitude that decreases with increasing FA concentration (15). The present work shows that also inhibition of ribosome recycling gives rise to biphasic kinetics with distinct fast and slow phases (Figure 4A). The ultimate reason for the two phases in translation and recycling is that in each case
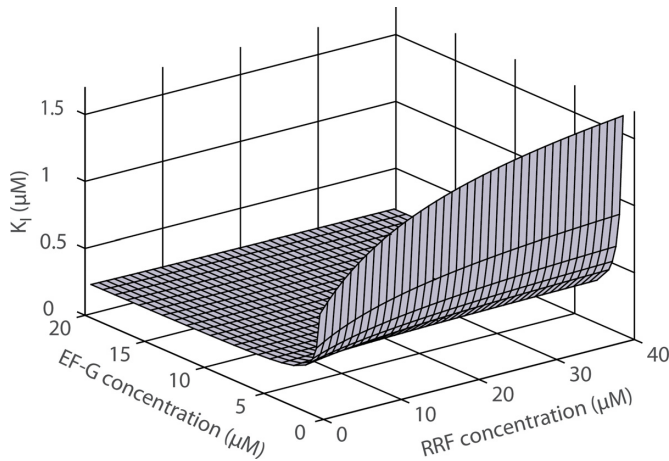
Figure 5. Dependence of the FA inhibition of ribosome recycling on the concentrations of RRF and EF-G. The K_I-value, the concentration of FA required to double the recycling time, given by Equation (5) plotted as a function of the EF-G (0.3–20 μM) and RRF (1–40 μM) concentrations.

the time of FA dissociation from ribosome-bound EF-G is much longer than the time to complete the corresponding unhindered process. There are two main reasons for paying attention to the existence of fast and slow phases in enzyme inhibition. The first is that by taking the two distinct phases into account one can extend the set of determinable parameters. The second is that the 'rugged' kinetics that results from the kinetic phases may have profound effects on growth inhibition of bacterial populations.

The scheme in Figure 1 can be described as a system of linear ordinary differential equations. The solution to such a system, which describes the product accumulation, can always be described as a sum of exponential terms ($y(t) = a_1(1-e^{-\lambda_1 t})+\ldots+a_n(1-e^{-\lambda_n t})$) with amplitudes ($a_1$ to a_n) and exponential coefficients, the eigenvalues (λ_1 to λ_n). For slow inhibitors, such as FA, one obtains a set of terms with slow eigenvalues and a set of terms with fast eigenvalues. The distinction between fast and slow eigenvalues can be made for all inhibitors with a slow dissociation rate from their inhibited ribosomal states in comparison to the rate of the uninhibited reaction. The kinetics of product accumulation in the presence of a slow inhibitor can thus be divided into a fast-reacting fraction with amplitude f_F and average time τ_F and a slowly reacting fraction with amplitude f_S ($= 1 - f_F$) and average time τ_S. Here f_F and f_S are the sums of the amplitudes connected to the fast and the slow eigenvalues, respectively. The average total time of product accumulation in ribosome recycling in the presence of FA (τ_{recFA}) can thus be obtained as (see also Equation (2)):

$$\tau_{recFA} = \tau_{rec} + \tau_{recI} = f_F\tau_F + f_S\tau_S \tag{7}$$

The average time of the fast phase decreased as the fast phase amplitude decreased upon FA addition, and was therefore approximated as: $\tau_F = \tau_{rec} \cdot f_F$. The parameters τ_{rec}, f_S and τ_S were estimated by fitting Equation (S4) (Supporting Material) to time traces for ribosome recycling obtained from experiments performed in parallel in the absence and presence of FA (Figure 4A). The slow phase amplitude, f_S, was used to approximate the probability, p_I, in

Equation (7) that a ribosome undergoing recycling was inhibited by FA. The slow phase time, τ_S, was used to estimate the time increase, τ_I, to recycle an inhibited compared to an uninhibited ribosome as described above through: $\tau_S = \tau_I + (1+f_F)\tau_{rec}$. From this we obtain:

$$\tau_{recFA} = \tau_{rec} + \tau_{recI} = \tau_{rec} + p_I\tau_I \tag{8}$$

Equation (8) is an approximation that becomes better with decreasing τ_{rec}/τ_I ratio, and thus can be very precise for slow inhibitors like FA (15), viomycin (21) and others (22).

The experimentally estimated p_I-value responded hyperbolically to the FA concentration with a sensitivity that increased with increasing [EF-G]/[RRF] concentration ratio (Figure 4B), due to increased propensity of forming the $R_{G(GDP)\cdot FA}$ complex (Figure 1). The inhibition probability, p_I, is given by (Equation (S9)):

$$p_I = \frac{w\,[FA]}{(1+w)\,[FA] + K_{I1}} \cdot \frac{K_{I2}}{[FA] + K_{I2}} + \frac{[FA]}{[FA] + K_{I2}} \tag{9}$$

where

$$w = \frac{(k_{cat}/K_M)_{G1}}{k_{RRF}\,[RRF]}\left([G] + Q\left(1 + \frac{q_{G2}}{k_{split}}\frac{K_{I2}}{[FA] + K_{I2}}\right)\bigg/\left(1 + \frac{q_{G2}}{k_{split}}\right)\right) \tag{10}$$

The inhibition constants K_{I1} ($= q_{G1}/k_{FA1}$) and K_{I2} ($= k_{split}/k_{FA2}$) are defined as the ratios between the forward rate constant for leaving each one of the two FA susceptible states and their respective FA binding rate constants (Table 1). We note that the parameter w depends only weakly on the FA concentration since $q_{G1}/k_{split} << 1$ (Table 2). From Equations (2) and (8) it is seen that the extra delay time (τ_I) conferred by FA inhibition can be derived by dividing τ_{recI} with p_I: $\tau_I = \tau_{recI}/p_I$ (Equation (S10)). The τ_I-value was linear in the FA concentration with positive slope at all combinations of EF-G and RRF concentrations (Figure 4C). The y-axis intercepts (Equation (S11)), which reflect the average time of FA release after each binding event, were in all cases ~5 s, suggesting that the rate of release of FA from EF-G was similar in the absence and presence of RRF on the ribosome (Figure 1). The slope of the τ_I dependence on [FA] increased with increasing [EF-G]/[RRF] concentration ratio due to the increasing propensity of rebinding of EF-G and FA to the RRF-free post-termination complex (Figure 4C).

The elemental rate constants and Michaelis-Menten parameters in Table 2 were estimated by fitting all parameters in the recycling model Equations (1), (2) and (9) to all recycling times, τ_{recFA}, obtained without (19) and with (Figures 2B and 4D) FA, as well as to the inhibition probabilities, p_I (Figure 4B). τ_{recFA} and p_I could be expressed exclusively in terms of A-parameters and parameters related to FA inhibition (K_{I1}, K_{I2}, q_{FA1}), except for the ratio q_{G2}/k_{split} which was weighted into the fit by its mean value estimate and error (0.1 ± 0.1) which was known ((19), Table 2). We note that access to the p_I estimates was essential for obtaining estimates of the FA dissociation rate constants q_{FA1} and q_{FA2} from ribosomal states $R_{G(GDP)\cdot FA}$ and $R_{RRF\cdot G(GDP)\cdot FA}$, respectively, as well as the inhibition constants K_{I1} and K_{I2}. The reason is that each one of these dissociation rate constants appears multiplied with its corresponding inhibition constant (K_{I1} and K_{I2}, respectively) in the expressions for

the parameters A_6 and A_7 (Table 1). The spectrum of p_I-values (Figure 4B), as modelled by Equation (9), allowed separate K_I-value estimates ($K_{I1} = 13 \pm 14$ μM and $K_{I2} = 19 \pm 7$ μM) and FA release rate constant estimates ($q_{FA1} = 0.17 \pm 0.03$ s^{-1} and $q_{FA2} = 0.18 \pm 0.08$ s^{-1}).

The new estimates of the A_1–A_7 parameters obtained by this extended fitting procedure were virtually identical to those obtained above by fitting of the total recycling time Equations (1) and (2) to experimental data ((19) and Figures 2B and 4D) without consideration of the extra information buried in the p_I-values (Table 1). In general, single turnover experiments involving slowly dissociating inhibitors, giving rise to two distinct kinetic phases, are more information rich than those involving rapidly dissociating inhibitors (15,21,22). Furthermore, since slow inhibitors give rise to queuing of trailing ribosomes behind a stalled leading ribosome they are expected to display a different intracellular inhibition pattern than rapidly equilibrating, fast inhibitors (see Discussion).

Modelling of growth rate reduction by FA inhibition of peptide elongation and ribosome recycling

In this section we inspect FA-induced growth rate reduction of bacterial populations. We use the kinetics data obtained in the present and in previous work for FA inhibition of ribosome recycling (Table 1) and mRNA translocation (15), respectively, to model the impact of FA on bacterial growth. Simple global modelling of the double action of FA on translocation and on ribosome recycling suggests the generation (doubling) time, τ_G, to depend on the free concentration of FA, [FA], as (Supporting Material, Equations (S13)–(S15)):

$$\tau_G([FA]) = \tau_{eFA}\left(1 + \frac{\tau_{recFA}}{\tau_{eFA}N_P}\right)\frac{\ln 2 \cdot \rho_0}{[R_T]} = \tau_{eFA}(1+r)\frac{\ln 2 \cdot \rho_0}{[R_T]} \quad (11)$$

Here, τ_{recFA} is the ribosome recycling time given in Equations (1) and (2) with corresponding A-parameters in Table 1, τ_{eFA} is the peptide elongation cycle time, N_P ($= 400$) approximates the average number of amino acid residues per protein, $[R_T]$ is the total intracellular ribosome concentration and ρ_0 the intracellular concentration of amino acid residues (peptide bonds) in the proteome. We note that during synthesis of a protein there are N_P mRNA translocation events, all of which are putative targets for FA action, but only one recycling event. This fundamental difference between the two inhibition modes is accounted for by the presence of N_P in Equation (11). The parameter r ($= \tau_{recFA}/(\tau_{eFA}N_P)$) compares the growth inhibitory impact of FA on elongation with that on ribosome recycling. This comparison is useful for addressing a recent controversy (15) of whether FA action is dominated by inhibition of ribosome recycling, as previously suggested (4), or by inhibition of peptide elongation. When r is smaller than 1, the doubling time, τ_G, is dominated by τ_{eFA}, i.e. by elongation, but when r is larger than 1, τ_G is dominated by τ_{recFA}/N_P, i.e. by ribosome recycling.

The FA-inhibited ribosome recycling time, τ_{recFA}, is given by Equations (1) and (2), with A-parameters from Table 1. The FA-inhibited elongation cycle time, τ_{eFA}, is given by
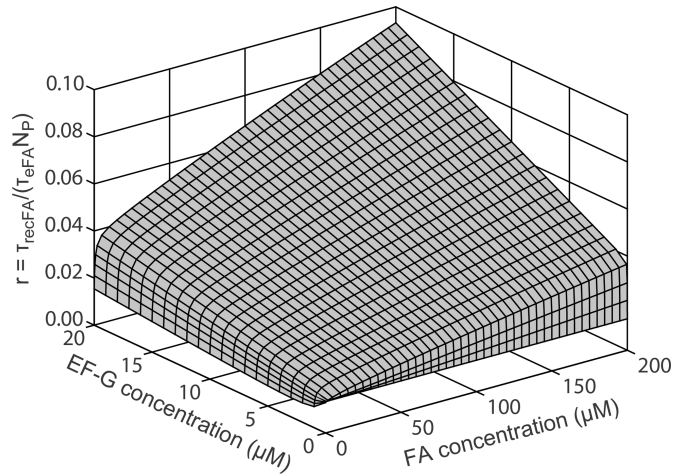
Figure 6. Contribution from the recycling step to the total time for synthesis of a protein of average size in the presence of FA. The ratio between the time spent in recycling and in elongation, $r = \tau_{recFA}/(\tau_{eFA}N_P)$ Equation (13), was plotted as a function of the free FA (0–200 μM) and EF-G (0–20 μM) concentrations at fixed RRF concentration (15 μM). The following parameters were used in Equation (13) to create the plot: $N_P = 400$, $\tau_{emin} = 0.05$ s, $(k_{cat}/K_M)_G = 30$ μM^{-1}s^{-1} (23), $1/q_{F2} = 9$ s, $1/q_{F3} = 6.1$ s and $K_{I1} = 120$ μM, $K_{I2} = 3.5$ mM and $K_{I3} = 2.8$ mM. For the recycling time we used Equation (2) and A-parameters from Table 1.

(15):

$$\tau_{eFA} = \tau_{Tu} + \left(\frac{K_M}{k_{cat}}\right)_G \frac{1}{[G]} + \tau_{e\,min\,G} + \left\{\frac{1}{q_{F2}}\frac{1}{[FA]+\kappa_{I1}} + \frac{1}{q_{F2}\kappa_{I2}} + \frac{1}{q_{F3}\kappa_{I3}}\right\}[FA] \quad (12)$$

The first term in Equation (12), τ_{Tu}, is the average time from after dissociation of EF-G from the post-termination ribosome to and including EF-Tu release after peptide bond formation. The second term is the effective time for EF-G binding to the pre-translocation ribosome with a peptidyl-tRNA in the A site. It may be pointed out that this term will increase with increasing FA concentration due to increasing EF-G sequestration on ribosomes, reducing the free EF-G concentration, [G]. The third term, τ_{eminG}, is the time required for an already ribosome-bound EF-G to translocate and dissociate from the post-translocation ribosome. The last term in Equation (12) is the increase in τ_{eFA} due to FA binding to EF-G on the translocating ribosome as determined by inhibition constants κ_{I1} ($= 120$ μM), κ_{I2} ($= 3.5$ mM) and κ_{I3} ($= 2.8$ mM), respectively (15). Parameters q_{F2} ($= 0.11$ s^{-1}) and q_{F3} ($= 0.16$ s^{-1}) are rate constants for FA dissociation from EF-G, bound to either one of two ribosome stalling states (15).

With Equations (1) and (2) for τ_{recFA} and Equation (12) for τ_{eFA} the impact ratio, r, in Equation (11) follows as:

$$r = \frac{1}{N_P}\frac{A_1 + A_2\frac{1}{[RRF]} + A_3\frac{[G]}{[RRF]} + A_4\frac{1}{[G]} + A_5\frac{1}{[RRF][G]} + (Q+[G])\cdot A_6\frac{[FA]}{[RRF]} + A_7[FA]}{\tau_{e\,min} + \left(\frac{K_M}{k_{cat}}\right)_G\frac{1}{[G]} + \left\{\frac{1}{q_{F2}}\frac{1}{[FA]+\kappa_{I1}} + \frac{1}{q_{F2}\kappa_{I2}} + \frac{1}{q_{F3}\kappa_{I3}}\right\}[FA]} \quad (13)$$

Here τ_{emin} is the sum of τ_{Tu} and τ_{eminG}. We used Equation (13) to calculate the impact ratio, r, for different free concentrations of FA (0–200 μM) and EF-G (0–20 μM) at a constant free concentration of RRF, 15 μM (Figure 6). It is

seen that for proteome synthesis with peptide chains of an average amino acid residue number, N_P, of 400 the ratio r remains below 10% at all these combinations of free FA and EF-G concentrations. In the range of what we consider as physiological concentrations of FA, EF-G and RRF, therefore, FA inhibition of peptide elongation rather than of ribosome recycling provides the dominant growth inhibitory impact of FA in living cells.

To zoom in on the details of how the r-value changes with the FA concentration we note that when the [FA]-dependent terms in Equation (13) dominate over the [FA] independent terms, the impact ratio, r, is approximated by

$$r = \frac{1}{N_P} \frac{(Q + [G]) \cdot \frac{A_6}{[\text{RRF}]} + A_7}{\left\{ \frac{1}{q_{F2}} \frac{1}{[\text{FA}] + \kappa_{I1}} + \frac{1}{q_{F2}\kappa_{I2}} + \frac{1}{q_{F3}\kappa_{I3}} \right\}} \quad (14)$$

Since we know that $\kappa_{I1} << \kappa_{I2} \approx \kappa_{I3}$ and $q_{F2} \approx q_{F3}$ it is seen that the r-value increases almost hyperbolically with increasing [FA]-concentrations above κ_{I1}. The r-value also increases with decreasing free concentration of RRF and increasing free concentration of EF-G. However, at high FA concentration, anomalously high EF-G concentration and anomalously low RRF concentration, FA inhibition of ribosome recycling may provide a growth inhibitory impact significant compared to that of elongation.

In the living cell it is normally the total concentrations of factors and ribosomes that are known. RRF has low affinity to the ribosome (19), and it is therefore reasonable to approximate the free with the total RRF concentration, [RRF$_T$]. It is then possible to derive the free EF-G concentration as one of the roots of a cubic equation ('Materials and Methods'). However, the K$_M$-value for the EF-G-ribosome interaction is comparatively small (23) and decreases with increasing FA concentration. When the total EF-G concentration, [G$_T$], is significantly larger than the total ribosome concentration, [R$_T$], a reasonable approximation is therefore to set [G] = [G$_T$] - [R$_T$] in Equation (13).

DISCUSSION

Ribosome recycling is the final stage of protein synthesis. Here a terminated ribosome is split into its small (30S) and large (50S) subunits by the concerted actions of RRF and EF-G (24), thereby making the subunits available for a new round of initiation (2). The basic outline of the recycling process and its FA susceptibility are known (4), but major mechanistic and quantitative aspects have remained obscure. Among these has been the lack of a reliable assessment of the relative contributions of FA-dependent inhibition of peptide elongation and of ribosome recycling to the inhibition of translation, and hence of the bacterial growth rate (15).

Building on our previous analysis of the mechanism of ribosome recycling (19), we now present a complete kinetic model of FA inhibition of the recycling process (Figure 1). The model, which predicts the mean time of ribosome recycling for all combinations of free concentrations of EF-G, RRF and FA, has been extensively corroborated by quench-flow and stopped-flow experiments (Figures 2, 3 and 4). Through our kinetic analysis we identify and quantify two distinct modes by which FA inhibits the recycling process.

Firstly, FA locks EF-G on the RRF-free post-termination ribosome, preventing binding of RRF until FA has dissociated from EF-G and then EF-G has dissociated from the ribosome. Secondly, when both RRF and EF-G are bound to the ribosome in a splitting-competent complex, FA binding prevents ribosome splitting by locking EF-G in an intermediate state on the splitting pathway (Figure 1). The dissolution of this pre-splitting complex into subunits begins as soon as FA has dissociated from EF-G, as demonstrated by kinetic experiments showing that the GTP consumption per ribosome splitting event is independent of the FA concentration (Figure 3). In other words, a ribosome complex containing both RRF and EF-G that has been stalled by FA remains primed for ribosome splitting all the time until FA has dissociated. This finding was unexpected since other possible scenarios appeared quite plausible. It could, for instance, be that the ribosome-bound RRF·EF-G(GDP)·FA complex undergoes a conformational change so that when FA dissociates the RRF·EF-G(GDP) complex cannot anymore induce ribosome splitting. In that case ribosome splitting would require EF-G dissociation followed by rebinding of another EF-G(GTP) to the RRF-containing ribosome at the free energy cost of hydrolysis of an extra GTP molecule.

We have seen that the average recycling time increases linearly with the FA concentration (Figure 4D), in sharp contrast to the non-linear increase in the peptide elongation cycle time in response to FA (12). In the recycling case, a ribosome that has been stalled by FA remains in the same state during the subsequent FA dissociation and re-association events that prolong the stalling time. This is the explanation for the linear increase in the average recycling time with increasing FA concentration ('Materials and Methods'). In contrast, in the elongation case, most ribosomes are first attacked by FA in an early state of the translocation process. Still drug-bound the ribosomes rapidly move on to a downstream state in which they are stalled. Subsequent drug dissociation and re-association events that prolong the stalling time occur in the downstream state, where drug association is much less efficient, which explains the non-linear response of the average elongation cycle time to the FA concentration (15).

Detailed kinetic analysis of the biphasic time curves of ribosome splitting obtained at varying concentrations of RRF, EF-G and FA (Figure 4A) was used to estimate the fraction of FA-bound ribosomes as well as the average time that they stay inhibited, due to slow FA dissociation and subsequent FA rebinding. Using this information we estimated all the inhibition and rate constants related to FA association to and dissociation from EF-G during ribosome recycling (Table 2). In the post-termination complex FA stays bound to EF-G for ∼5 s, both in the presence and absence of RRF, similar to the 9 and 6 s observed for FA binding to EF-G in the intermediate translocation state and in the post-translocation state, respectively (15). The efficiencies by which FA binds to the FA-susceptible states of the ribosome are smaller in translocation than in recycling: 50% probability of inhibition was obtained at ∼100 μM and ∼10 μM, respectively. This difference may be due to shorter lifetime of the states susceptible to FA association in translocation than in recycling.

Due to the lack of detailed knowledge of the kinetics of ribosome recycling, it has previously not been possible to obtain a homologous structure of EF-G and RRF bound simultaneously to the 70S ribosome, not even in the presence of FA. However, a two-factor structure has been obtained with EF-G from *E. coli* and RRF from *Thermus thermophilus* (25). Since, however, this heterologous EF-G and RRF pair is inactive in ribosome recycling (26,27), the functional relevance of this ribosome complex is unclear. The present results show that (i) FA stalls the ribosome in a splitting-primed state containing both RRF and EF-G; (ii) the stalling time can be made long enough to be compatible with the sample preparation times required for classical cryo-EM methods simply by using a sufficiently high FA concentration. An alternative approach to determine the structure of the RRF- and EF-G-bound complex with or without FA would be to use time-resolved cryo-EM methods, currently under development (28,29), that allow incubation in the millisecond time range before freezing of the sample on the EM-grid.

It has been suggested that FA inhibition of ribosome recycling rather than peptide elongation is the main contributing factor to the growth inhibiting effect of the drug (4). This assertion was based on a comparison of the K_I-value for recycling, estimated as 0.1 μM, and the K_I-value for translocation, estimated as 200 μM. From this followed the seemingly natural conclusion that FA inhibition of ribosome recycling, with its 2000-fold higher FA sensitivity, must be the major growth inhibitory factor. However, due to suboptimal experimental design, the K_I-value for translocation had been overestimated almost 400-fold and was actually around 0.6 μM (15). When, furthermore, it is taken into account that there is but one recycling event and ~400 protein translocation events in the making of an average bacterial protein, a different scenario emerges. Taking advantage of our previous quantitative analysis of FA inhibition of the translocation cycle (15) and the present observations of FA inhibition of ribosome recycling we have used estimates of the free concentrations *in vivo* of RRF (15 μM, (30,31)) and EF-G (4 μM (15)) to assess the relative importance of FA inhibition of protein elongation and recycling for bacterial growth reduction (Figure 6). We find that under normal physiological conditions and intracellular FA concentrations below 200 μM, <10% of the growth inhibition can be ascribed to recycling and >90% to translocation. However, under anomalous conditions of RRF deficiency or excess synthesis of EF-G, inhibition of ribosome recycling may become a significant growth inhibitory factor.

Even though FA inhibition of ribosome recycling has a relatively small effect on the time to translate a bacterial protein of average size, it may have larger impact on translation of short open reading frames (ORFs). For example, at 4 μM EF-G, 15 μM RRF and 20 μM FA a ribosome translating a 400 codon ORF spends <3% of its time in the recycling phase, whereas for a 20 codon ORF the recycling time constitutes as much as 33% of the total synthesis time Equation (13). An interesting case may be the induction of the synthesis of the plasmid-encoded resistance protein FusB, which is believed to disassemble FA-stalled ribosome complexes and thereby reduce the FA sensitivity of the bacterial strain (9). The expression of FusB is controlled by translational attenuation (32), in a manner reminiscent of some macrolide resistance mechanisms (33). The FusB gene is preceded by a short ORF encoding a 20 amino acid leader peptide (32). Stalling of ribosomes by FA during synthesis of the leader peptide leads to rearrangement of the mRNA secondary structure and exposure of the ribosome binding site for FusB translation (32). We suggest that a large fraction of the ribosomes are stalled at the stop codon of the short leader ORF, due to FA inhibition of ribosome recycling.

Finally, we note that since FA is a slow inhibitor with residence times of about 5–10 s both in translocation and recycling, its binding may cause ribosomal queuing on translated mRNAs. More precise modelling of the growth inhibitory effects of FA will therefore require that ribosome queuing and other pertinent effects are taken into account.

SUPPLEMENTARY DATA

Supplementary Data are available at NAR Online.

REFERENCES

1. Schmeing,T.M. and Ramakrishnan,V. (2009) What recent ribosome structures have revealed about the mechanism of translation. *Nature*, **461**, 1234–1242.
2. Karimi,R., Pavlov,M.Y., Buckingham,R.H. and Ehrenberg,M. (1999) Novel roles for classical factors at the interface between translation termination and initiation. *Mol. Cell*, **3**, 601–609.
3. Hirokawa,G., Nijman,R.M., Raj,V.S., Kaji,H., Igarashi,K. and Kaji,A. (2005) The role of ribosome recycling factor in dissociation of 70S ribosomes into subunits. *RNA*, **11**, 1317–1328.
4. Savelsbergh,A., Rodnina,M.V. and Wintermeyer,W. (2009) Distinct functions of elongation factor G in ribosome recycling and translocation. *RNA*, **15**, 772–780.
5. Godtfredsen,W.O., Jahnsen,S., Lorck,H., Roholt,K. and Tybring,L. (1962) Fusidic acid: a new antibiotic. *Nature*, **193**, 987.
6. Johanson,U. and Hughes,D. (1994) Fusidic acid-resistant mutants define three regions in elongation factor G of Salmonella typhimurium. *Gene*, **143**, 55–59.
7. Nagaev,I., Bjorkman,J., Andersson,D.I. and Hughes,D. (2001) Biological cost and compensatory evolution in fusidic acid-resistant Staphylococcus aureus. *Mol. Microbiol.*, **40**, 433–439.
8. Norstrom,T., Lannergard,J. and Hughes,D. (2007) Genetic and phenotypic identification of fusidic acid-resistant mutants with the small-colony-variant phenotype in Staphylococcus aureus. *Antimicrob. Agents Chemother.*, **51**, 4438–4446.
9. Cox,G., Thompson,G.S., Jenkins,H.T., Peske,F., Savelsbergh,A., Rodnina,M.V., Wintermeyer,W., Homans,S.W., Edwards,T.A. and O'Neill,A.J. (2012) Ribosome clearance by FusB-type proteins mediates resistance to the antibiotic fusidic acid. *Proc. Natl. Acad. Sci. U. S. A.*, **109**, 2102–2107.
10. Guo,X., Peisker,K., Backbro,K., Chen,Y., Koripella,R.K., Mandava,C.S., Sanyal,S. and Selmer,M. (2012) Structure and function of FusB: an elongation factor G-binding fusidic acid resistance protein active in ribosomal translocation and recycling. *Open Biol.*, **2**, 120016.

11. Okura,A., Kinoshita,T. and Tanaka,N. (1971) Formation of fusidic acid-G factor-GDP-ribosome complex and the relationship to the inhibition of GTP hydrolysis. *J. Antibiot. (Tokyo)*, **24**, 655–661.

12. Burdett,V. (1996) Tet(M)-promoted release of tetracycline from ribosomes is GTP dependent. *J. Bacteriol.*, **178**, 3246–3251.

13. Willie,G.R., Richman,N., Godtfredsen,W.P. and Bodley,J.W. (1975) Some characteristics of and structural requirements for the interaction of 24,25-dihydrofusidic acid with ribosome - elongation factor g Complexes. *Biochemistry (Mosc)*, **14**, 1713–1718.

14. Bodley,J.W., Zieve,F.J. and Lin,L. (1970) Studies on translocation. IV. The hydrolysis of a single round of guanosine triphosphate in the presence of fusidic acid. *J. Biol. Chem.*, **245**, 5662–5667.

15. Borg,A., Holm,M., Shiroyama,I., Hauryliuk,V., Pavlov,M., Sanyal,S. and Ehrenberg,M. (2015) Fusidic acid targets elongation factor G in several stages of translocation on the bacterial ribosome. *J. Biol. Chem.*, **290**, 3440–3454.

16. Ramrath,D.J., Lancaster,L., Sprink,T., Mielke,T., Loerke,J., Noller,H.F. and Spahn,C.M. (2013) Visualization of two transfer RNAs trapped in transit during elongation factor G-mediated translocation. *Proc. Natl. Acad. Sci. U.S.A.*, **110**, 20964–20969.

17. Gao,Y.G., Selmer,M., Dunham,C.M., Weixlbaumer,A., Kelley,A.C. and Ramakrishnan,V. (2009) The structure of the ribosome with elongation factor G trapped in the posttranslocational state. *Science*, **326**, 694–699.

18. Zavialov,A.V., Hauryliuk,V.V. and Ehrenberg,M. (2005) Splitting of the posttermination ribosome into subunits by the concerted action of RRF and EF-G. *Mol. Cell*, **18**, 675–686.

19. Borg,A., Pavlov,M. and Ehrenberg,M. (2016) Complete kinetic mechanism for recycling of the bacterial ribosome. *RNA*, **22**, 10–21.

20. Johansson,M., Bouakaz,E., Lovmar,M. and Ehrenberg,M. (2008) The kinetics of ribosomal peptidyl transfer revisited. *Mol. Cell*, **30**, 589–598.

21. Holm,M., Borg,A., Ehrenberg,M. and Sanyal,S. (2016) Molecular mechanism of viomycin inhibition of peptide elongation in bacteria. *Proc. Natl. Acad. Sci. U.S.A.*, **113**, 978–983.

22. Lovmar,M., Tenson,T. and Ehrenberg,M. (2004) Kinetics of macrolide action: the josamycin and erythromycin cases. *J. Biol. Chem.*, **279**, 53506–53515.

23. Borg,A. and Ehrenberg,M. (2015) Determinants of the rate of mRNA translocation in bacterial protein synthesis. *J. Mol. Biol.*, **427**, 1835–1847.

24. Janosi,L., Hara,H., Zhang,S. and Kaji,A. (1996) Ribosome recycling by ribosome recycling factor (RRF)–an important but overlooked step of protein biosynthesis. *Adv. Biophys.*, **32**, 121–201.

25. Yokoyama,T., Shaikh,T.R., Iwakura,N., Kaji,H., Kaji,A. and Agrawal,R.K. (2012) Structural insights into initial and intermediate steps of the ribosome-recycling process. *EMBO J.*, **31**, 1836–1846.

26. Raj,V.S., Kaji,H. and Kaji,A. (2005) Interaction of RRF and EF-G from E. coli and T. thermophilus with ribosomes from both origins–insight into the mechanism of the ribosome recycling step. *RNA*, **11**, 275–284.

27. Ito,K., Fujiwara,T., Toyoda,T. and Nakamura,Y. (2002) Elongation factor G participates in ribosome disassembly by interacting with ribosome recycling factor at their tRNA-mimicry domains. *Mol. Cell*, **9**, 1263–1272.

28. Shaikh,T.R., Yassin,A.S., Lu,Z., Barnard,D., Meng,X., Lu,T.M., Wagenknecht,T. and Agrawal,R.K. (2014) Initial bridges between two ribosomal subunits are formed within 9.4 milliseconds, as studied by time-resolved cryo-EM. *Proc. Natl. Acad. Sci. U.S.A.*, **111**, 9822–9827.

29. Chen,B., Kaledhonkar,S., Sun,M., Shen,B., Lu,Z., Barnard,D., Lu,T.M., Gonzalez,R.L. Jr and Frank,J. (2015) Structural dynamics of ribosome subunit association studied by mixing-spraying time-resolved cryogenic electron microscopy. *Structure*, **23**, 1097–1105.

30. Andersen,L.D., Moreno,J.M., Clark,B.F., Mortensen,K.K. and Sperling-Petersen,H.U. (1999) Immunochemical determination of cellular content of translation release factor RF4 in Escherichia coli. *IUBMB Life*, **48**, 283–286.

31. Ishihama,Y., Schmidt,T., Rappsilber,J., Mann,M., Hartl,F.U., Kerner,M.J. and Frishman,D. (2008) Protein abundance profiling of the Escherichia coli cytosol. *BMC Genomics*, **9**, 102.

32. O'Neill,A.J. and Chopra,I. (2006) Molecular basis of fusB-mediated resistance to fusidic acid in Staphylococcus aureus. *Mol. Microbiol.*, **59**, 664–676.

33. Dubnau,D. (1984) Translational attenuation: the regulation of bacterial resistance to the macrolide-lincosamide-streptogramin B antibiotics. *CRC Crit. Rev. Biochem.*, **16**, 103–132.